Talanta 81 (2010) 813–818

Contents lists available at ScienceDirect

Talanta

journal homepage: www.elsevier.com/locate/talanta

Fabrication of Pt/polypyrrole hybrid hollow microspheres and their application in electrochemical biosensing towards hydrogen peroxide

Xiujie Bian, Xiaofeng Lu*, E. Jin, Lirong Kong, Wanjin Zhang, Ce Wang*

Alan G. MacDiarmid Institute, Jilin University, Changchun 130012, PR China

ARTICLE INFO

Article history:
Received 29 October 2009
Received in revised form 11 January 2010
Accepted 13 January 2010
Available online 21 January 2010

Keywords:
Pt nanoparticles
PPy
Electrocatalytic
Hydrogen peroxide reduction

ABSTRACT

Pt/polypyrrole (PPy) hybrid hollow microspheres were successfully prepared by wet chemical method via Fe_3O_4 template and evaluated as electrocatalysts for the reduction of hydrogen peroxide. The as-synthesized products were characterized by scanning electron microscopy (SEM), transmission electron microscopy (TEM), X-ray photoelectron spectra (XPS), X-ray diffraction (XRD), inductive coupled plasma emission spectrum (ICP) and Fourier-transform infrared spectra (FTIR) measurements. The results exhibited that ultra-high-density Pt nanoparticles (NPs) were well deposited on the PPy shell with the mean diameters of around 4.1 nm. Cyclic voltammetry (CV) results demonstrated that Pt/PPy hybrid hollow microspheres, as enzyme-less catalysts, exhibited good electrocatalytic activity towards the reduction of hydrogen peroxide in 0.1 M phosphate buffer solution (pH = 7.0). The composite had a fast response of less than 2 s with linear range of 1.0–8.0 mM and a relatively low detection limit of 1.2 μM (S/N = 3). The sensitivity of the sensor for H_2O_2 was 80.4 mA M^{-1} cm^{-2}.

1. Introduction

In the past decade, the investigation of hybrid nanomaterials has been one of the most extensively studied research areas for their combination of the different properties of each component. Among them, conducting polymers/metal hybrid nanomaterials have attracted more and more attention because of their various applications in catalysis, sensors and other aspects [1–4]. In the recent years, the rapid development of direct methanol fuel cells and biosensors affords the exploration of platinum (Pt) NPs and platinum-based nanostructures as electrocatalytic materials by taking advantage of their biocompatibility, huge surfaces and good electrocatalytic activity [5–10]. It is observed that the size and shape of the Pt NPs play an important role in their electrochemical catalytic properties [5,6]. The smaller are the Pt NPs (with higher surface-to-volume ratio), the more active catalytic properties do they have. Thus, the preparation of Pt NPs with diameters within 10 nm is of significance for their applications in electrocatalysis.

On the other hand, since their discovery, conducting polymers have received considering attention because of their high conductivity, good environmental stability and easy preparation. Furthermore, they have been proved good supporting matrixes for loading metal NPs [11–14]. The conducting polymers could not only inhibit the aggregation of metal NPs but also facilitate electron transfer which benefits for sensing sensitivity and selectivity. Among the conducting polymers, polypyrrole (PPy) has been long recognized as a promising member for application in electrocatalysis as well as for other purposes [15–17]. PPy has been successfully applied as the conducting matrixes of composite materials to incorporate noble metals such as Au, Ag, Pd, Ru and Pt [18–25]. Various nanostructures of PPy materials, such as films, nanograins and nanowires, were used as matrixes for supporting platinum NPs, which have been used as electrode materials, exhibiting good electrocatalytic activity towards the reduction of nitrite and the oxidation of methanol as well as glucose [22–25]. However, searching for an enhancing hybrid nanomaterial as electrochemical sensor for detecting H_2O_2 with high performance is still a challenge.

It is well known that H_2O_2 is not only the raw material of many industrial processes, but also the by-product of many biological oxidases reactions. Therefore, H_2O_2 detecting is very important in many different fields. Enzyme modified electrodes, especially horseradish peroxidase (HRP)-based electrodes, are frequently used for detecting relatively low concentrations of H_2O_2 [26–30]. However, they usually require rigorous environments, which could not endure at high temperature ranges, and do not have the lifetime of conventional noble metal catalysts. In addition, they usually need complicated immobilization procedure. Compared with enzyme modified electrodes, noble metal-based modified electrodes, which do not demand for rigorous environments, take on high sensitivity and good stability. Therefore, it is significative to develop new non-enzyme noble metal catalysts for H_2O_2. In this paper, we adopted the wet chemical methods to synthesize ultra-high-density Pt/PPy

* Corresponding authors. Tel.: +86 431 85168924; fax: +86 431 85168924.
E-mail addresses: xflu@jlu.edu.cn (X. Lu), cwang@jlu.edu.cn (C. Wang).

0039-9140/$ – see front matter © 2010 Elsevier B.V. All rights reserved.
doi:10.1016/j.talanta.2010.01.020

hybrid hollow microspheres using the Fe_3O_4 microspheres as template and extended them for biosensing applications. This method not only provides a simple and effective way to produce ultrahigh-density Pt NPs with large specific surface area, but also is proved to be one-pot approach to synthesize hybrid hollow spheres without post-treatment. The present results demonstrated that the obtained Pt/PPy hybrid hollow microspheres exhibited superior electrocatalytic activity towards the reduction of H_2O_2.

2. Experimental

2.1. Chemicals and reagents

Pyrrole was distilled under reduced pressure before use; other reactants including NaAc, ethylene glycol, poly (ethylene glycol) (Mw = 15,000), $FeCl_3{\cdot}6H_2O$, dodecyl sulfate sodium (SDS), formic acid and $H_2PtCl_6{\cdot}6H_2O$ were used as received without further purification. 0.1 M phosphate buffer solution (PBS, pH = 7.0) was prepared with 0.1 M Na_2HPO_4 and 0.1 M NaH_2PO_4, both of which contains 0.1 M NaCl. H_2O_2 aqueous solution was prepared freshly with 30% H_2O_2 just before use.

2.2. Experimental process

The synthesis of core-shell structured Fe_3O_4/PPy microspheres is the same as our previous work [31]. The mass ratio of pyrrole to Fe_3O_4 was fixed on 1:1. For the preparation of Pt/PPy hybrid hollow microspheres, the as-synthesized Fe_3O_4/PPy composite microspheres (0.018 g) were dispersed in 10 ml aqueous solution by ultrasonic irradiation for about 0.5 h. Then 10 ml solution containing 0.032 g $H_2PtCl_6{\cdot}6H_2O$ was added into the solution above. At last 1.0 ml formic acid was added into it to begin the reaction. The reaction was conducted under 80 °C in the water bath with mechanical stirring for half an hour. Refluxing conditions were used to keep the water in the synthesis system. Then heating was stopped and stirring was continued for 2 h. The obtained product was centrifuged and washed several times with water and ethanol, respectively. Finally the product was dried in vacuum at room temperature for 24 h.

2.3. Preparation and modification of electrodes

Prior to modification, the basal glassy carbon disk electrode (GCE) was polished with emery papers and slurries of alumina polishing powder to a mirror finish. After each polishing, the electrode was sonicated in ethanol and distilled water for 0.5 min, respectively, in order to remove any adhesive substances on the electrode surface. To modify the electrode, 4.5 μl Pt/PPy hybrid microspheres dispersion solution (5 mg/ml in ethanol) was mixed with 0.5 μl 5% Nafion (in ethanol). Then the mixture was sonicated about 10 min. Finally, the suspension was dropped on GCE surface and dried under ambient atmosphere.

2.4. Apparatus

The ultrasonic experiments were carried out by an ultrasonic disperser (KQ 50 B, Kunshan ultrasonic Instrument Co. Ltd. 40 kHz, 50 W). The structure of hybrid microspheres images were taken using scanning electron microscopy (SEM) and transmission electron microscopy (TEM). The SEM measurements were performed on a SHIMADZU SSX-550 microscope. TEM experiments were performed on a Hitachi H-800 microscope with an acceleration voltage of 200 kV. Analysis of the X-ray photoelectron spectra (XPS) were performed on an ESCLAB MKII measurements. FTIR spectra of KBr powder-pressed pellets were recorded on a Bruker Vertex 80v spectrometer. X-ray diffraction patterns (XRD) were obtained with a Siemens D5005 diffractometer using Cu Ka radiation. Inductive coupled plasma emission spectrum (ICP), used to detect the content of Pt and Fe elements in hollow Pt/PPy hybrid microspheres, was performed on emission spectrometer plasma 1000 (PerkinElmer). A Model CHI 660C electrochemical workstation was used for electrochemical measurements. A three-electrode electrochemical cell system was used. An Ag/AgCl electrode and a platinum wire electrode were used as the reference electrode and the counter electrode, respectively. A glassy carbon disk electrode (GCE, Φ3.0 mm) served as the basal working electrode. All electrochemical experiments were carried out at ambient temperature.

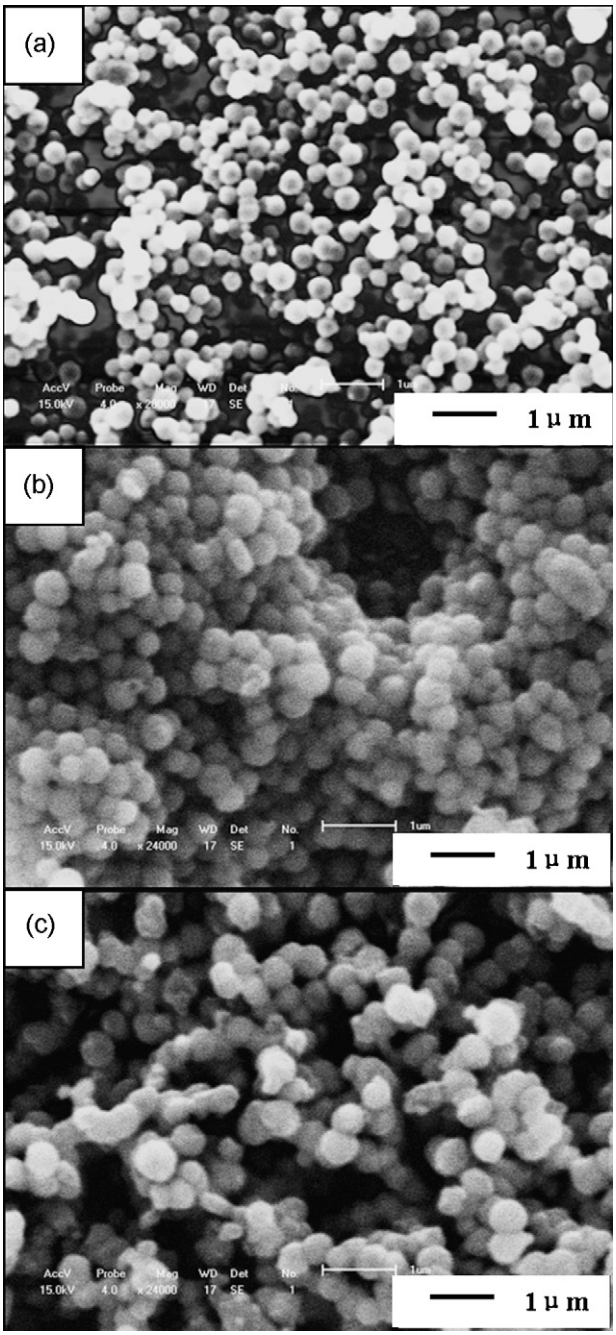

Fig. 1. SEM images of Fe_3O_4 spheres (a), Fe_3O_4/PPy composite spheres (b) and Pt/PPy composites (c).

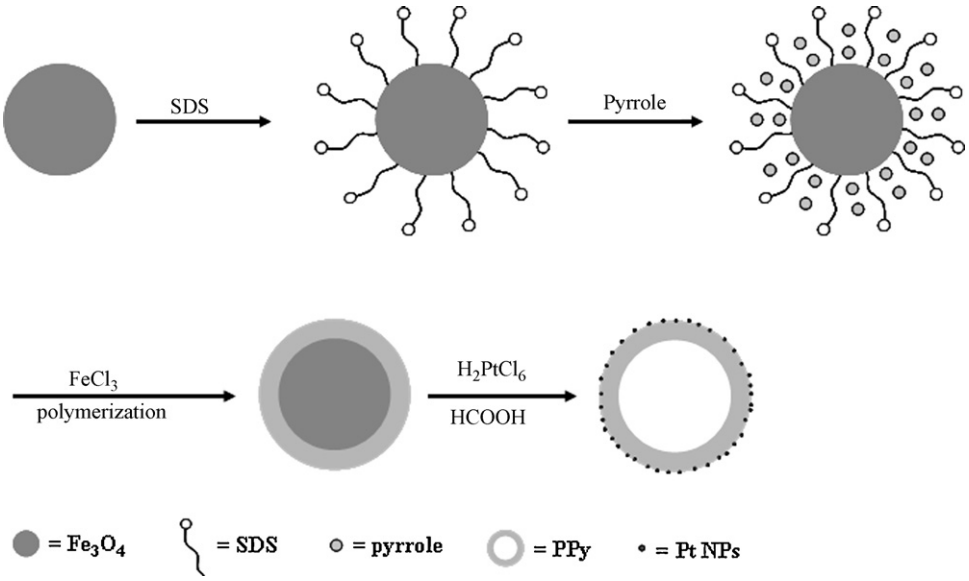

Scheme 1. Schematic of the preparation of Fe_3O_4/PPy composite and Pt/PPy hollow spheres.

3. Results and discussion

3.1. Chemical structure and composition characterization of hybrid materials

As illustrated in Scheme 1, the wet chemical approach for the fabrication of Pt/PPy hybrid microspheres using Fe_3O_4 microspheres as template involved two main steps. Firstly, the core-shell structured Fe_3O_4/PPy composite microspheres were prepared through chemical oxidation polymerization in the presence of anion surfactant. Then Pt NPs were decorated on the surface of PPy shells by reducing H_2PtCl_6 with HCOOH, meanwhile, the Fe_3O_4 core was dissolved by HCOOH and the H^+ produced by the polymerization process. The morphologies of the resulting products were investigated by SEM and TEM measurements. Fig. 1 shows typical SEM images of Fe_3O_4 microspheres, Fe_3O_4/PPy composite spheres and Pt/PPy hybrid microspheres. The results exhibited that all of the microspheres are uniform, smooth and regular spheres. TEM images (Fig. 2b) revealed the apparent core-shell-like morphology of Fe_3O_4/PPy composite microspheres. From the figure, it can be

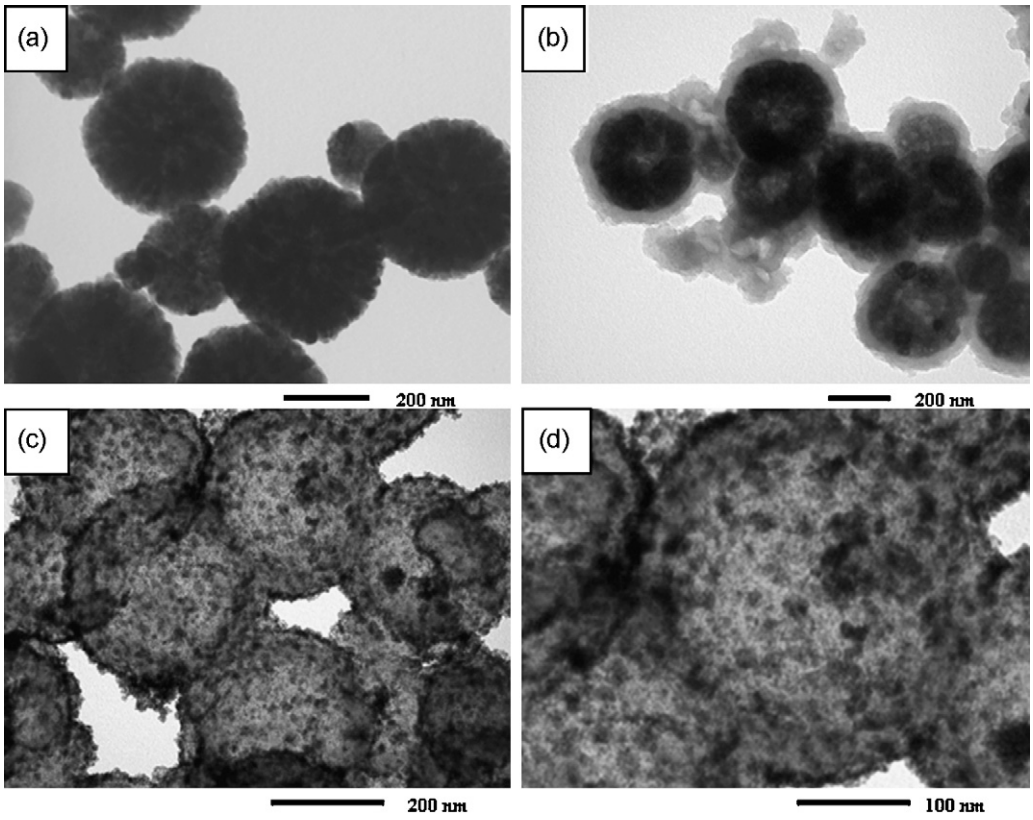

Fig. 2. TEM images of (a) Fe_3O_4 microspheres, (b) Fe_3O_4/PPy composites and (c and d) Pt/PPy hybrid spheres at different magnification.

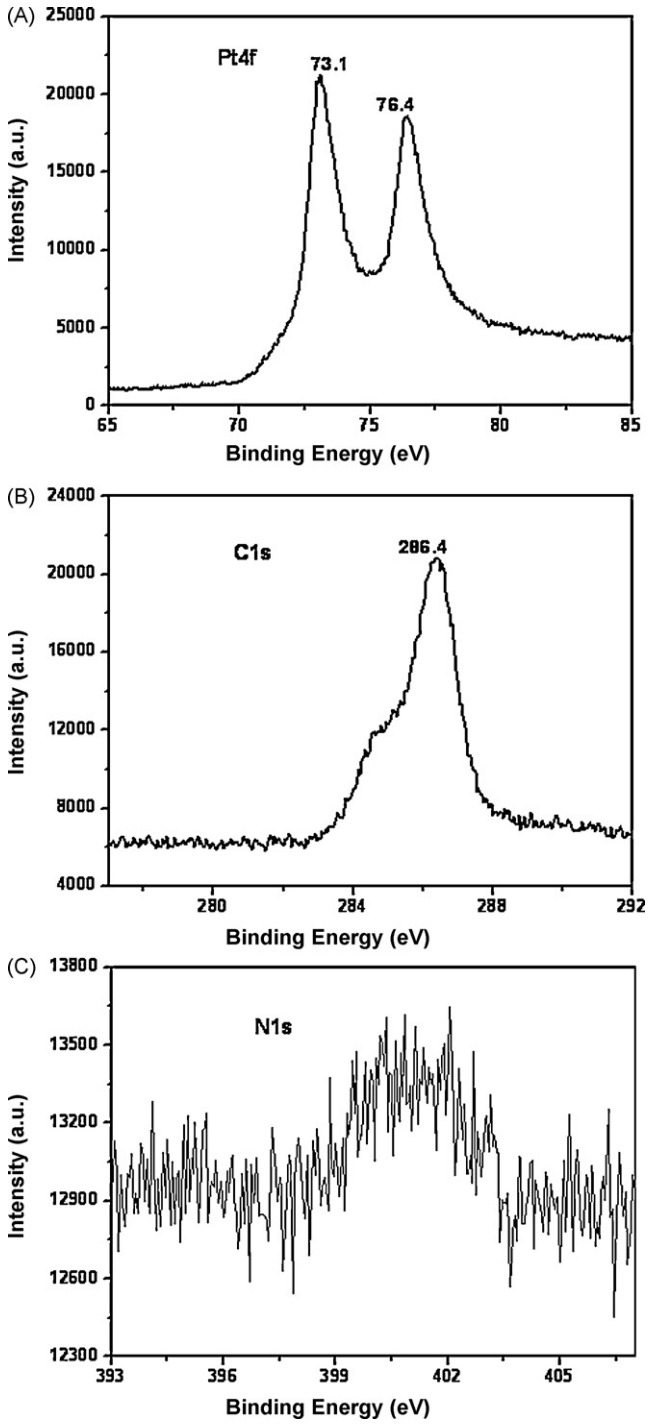

Fig. 3. XPS patterns of the Pt/PPy hybrid hollow spheres: (A) Pt4f; (B) C1s; (C) N1s.

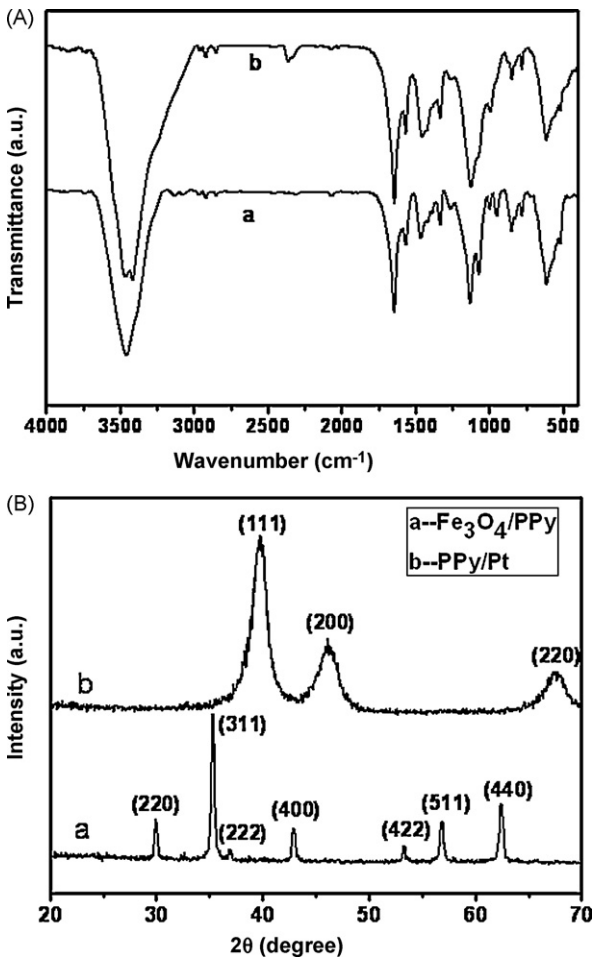

Fig. 4. (A) FTIR images and (B) X-ray diffraction pattern of (a) Fe_3O_4/PPy composites and (b) Pt/PPy hybrid hollow microspheres.

seen that the shell thickness of the Fe_3O_4/PPy composites is about 40–60 nm. After decoration with Pt NPs, the Fe_3O_4 core was dissolved, high density Pt NPs/PPy hybrid hollow microspheres were obtained, which have been clearly observed from TEM images in Fig. 2(c and d). The ICP results exhibited that the as-synthesized Pt/PPy hybrid hollow spheres only contained 1.763 wt% of Fe element, but contained 68.33 wt% of Pt element. These results are consistent with TEM images. In this paper, we adopted HCOOH as a reducing agent for preparing Pt NPs. Furthermore, the chemical polymerization of pyrrole will also produce large amount of H^+. So as the reaction proceeded, Fe_3O_4 core dissolved gradually under such strong acidic condition, leading to hollow spheres.

To confirm the existence of Pt and PPy in the resulting composites, an XPS experiment was employed for the surface analysis of the sample. XPS patterns (Fig. 3) of the obtained composites show a significant Pt4f signal corresponding to the binding energy of metallic Pt (Fig. 3A), a C1s signal corresponding to the binding energy of C (Fig. 3B), and a N1s signal corresponding to the binding energy of N (Fig. 3C). Thus, it was confirmed that Pt/PPy hybrid hollow spheres were obtained by the wet chemical method using Fe_3O_4 microspheres as template.

The molecular structure of the Pt/PPy hybrid hollow spheres was characterized by FTIR spectroscopy and XRD patterns. As shown in Fig. 4A, the characteristic bands of the Pt/PPy hybrid hollow spheres were the pyrrole ring fundamental vibration at 1564 cm^{-1} (C=C stretching) and 1456 cm^{-1} (C–C stretching), C–N stretching vibration in the ring and C–H deformation vibration at 1338 and 1068 cm^{-1}, respectively, C–C breathing at 1132 cm^{-1}, N–H stretching mode at 3461 cm^{-1} and a C–H out of plane vibration at 846 cm^{-1}. No obvious differences were found in FTIR spectra between the Pt/PPy hybrid hollow spheres and Fe_3O_4/PPy spheres, indicating that no chemical bonds exist between Pt NPs and PPy shell. Fig. 4B shows the X-ray diffraction pattern of the Fe_3O_4/PPy microspheres and Pt/PPy hybrid hollow spheres. All the diffraction peaks at 30.0°, 35.4°, 36.9°, 42.8°, 53.3°, 56.8° and 62.4° for Fe_3O_4/PPy microspheres are observed, which are in agreement with the XRD patterns of Fe_3O_4 microspheres. These peaks correspond to (2 2 0), (3 1 1), (2 2 2), (4 0 0), (4 2 2), (5 1 1) and (4 4 0) Bragg reflection of Fe_3O_4, respectively, indicating that the Fe_3O_4/PPy

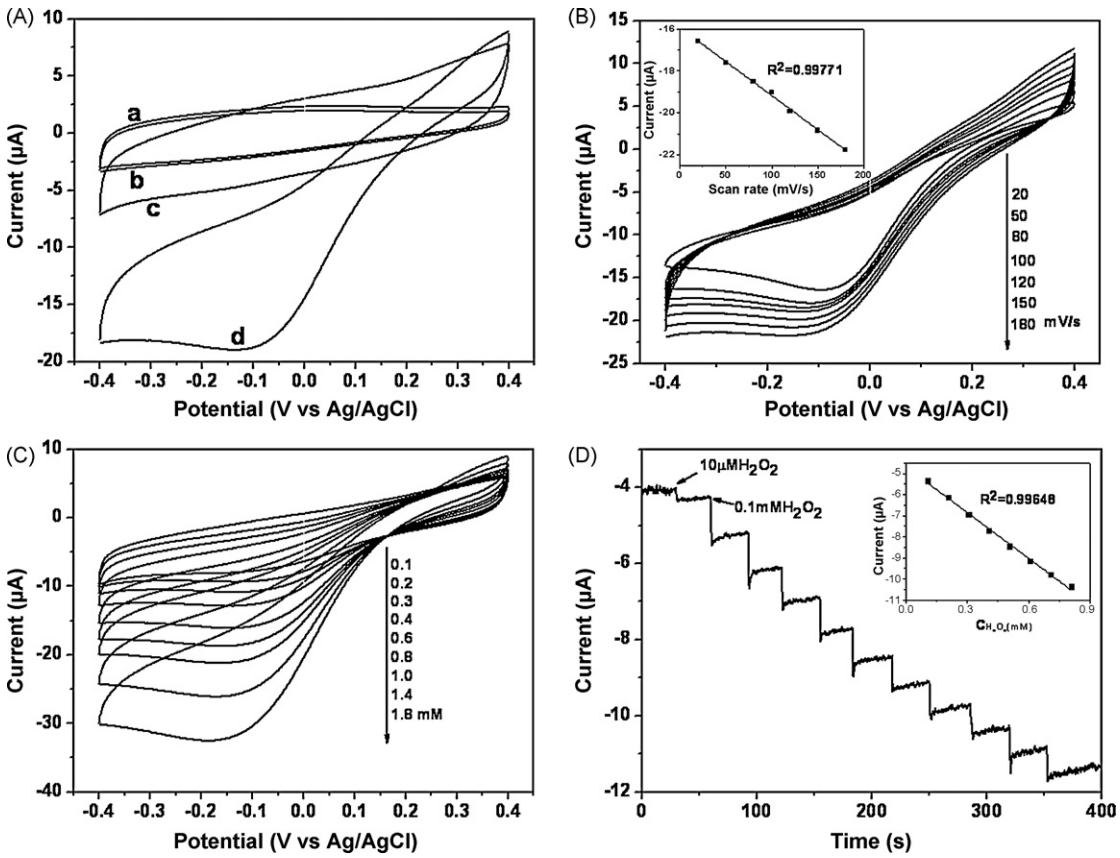

Fig. 5. (A) CVs of H_2O_2 reduction at the bare GCE (a and b) and GCE modified by Pt/PPy hybrid microspheres (c and d) in a 0.1 M PBS in the absence (a and c) and presence of 1.0 mM H_2O_2 (b and d). The scan rate is 100 mV/s. (B) CVs of modified GCE in 0.1 M PBS (pH = 7.0) in the presence of 1.0 mM H_2O_2 with different scan rate. The inset shows the calibration plot of reduction peak current of H_2O_2 verse scan rate. (C) CVs of modified GCE in 0.1 M PBS (pH = 7.0) in the presence of H_2O_2 with different concentrations. Scan rate: 100 mV/s. (D) Amperometric *i*–*t* curves of modified GCE at the constant potential of −0.1 V in 0.1 M PBS (pH = 7.0) with successive injection of H_2O_2. The inset shows the calibration plot of electrocatalytic current of H_2O_2 verse its concentrations.

composite microspheres contain Fe_3O_4 spheres. After decoration with Pt NPs, these peaks disappeared, indicating the dissolution of Fe_3O_4 core. The diffraction peaks at around 2θ of 39.7° (1 1 1), 46.2° (2 0 0) and 67.4° (2 2 0) for Pt/PPy hybrid hollow spheres could be assigned to the Pt face-centered cubic (fcc) structure. According to Scherrer's equation, $D_{hkl} = \kappa\lambda \times 57.3/\beta\cos\theta$, the average particle size of the deposited Pt-catalysts was calculated to be around 4.1 nm when the reflecting peaks of (1 1 1), (2 0 0) and (2 2 0) of the Pt cubic (fcc) lattice were chosen for calculating the crystal size of Pt.

3.2. Electrochemical performances of the Pt-PPy modified electrode towards hydrogen peroxide

The as-synthesized Pt/PPy hybrid hollow spheres were used as enzyme-less catalysts to modify electrode in order to study their electrocatalytic activities towards H_2O_2. From line (a and b) in Fig. 5A, it could be seen that bare GCE has little response to 1.0 mM H_2O_2 in 0.1 M PBS (only 0.323 μA increases in current and no reduction peak appears), which interprets that H_2O_2 reduction could not be achieved at bare GCE. While, it is obviously observed that a new peak occurs at around −0.1 V for the modified GCE (line d in Fig. 5A), which is attributed to the reduction of H_2O_2. The reduction peak current in the presence of 1.0 mM H_2O_2 is much larger than the current of GCE, indicating that the modified electrode exhibits good electrocatalytic activities towards H_2O_2. This is mainly attributed to the high electrocatalytic activity of the ultra-high-density Pt NPs deposited on PPy shell. Furthermore, we investigated the effect of scan rate on reduction peak current. As seen in Fig. 5B, the cathodic peak current, in the presence of 1.0 mM H_2O_2, increases with the increasing scan rate. The peak current increases linearly with the scan rate in the range of 20–180 mV/s (the inset of Fig. 5B), indicating that it is a surface-controlled process. It is well known that the hydrogen peroxide electroreduction can proceed through direct and indirect pathways. The direct reduction occurs via a two-electron process ($H_2O_2 + 2e^- \rightarrow 2OH^-$). The indirect reduction consists of the decomposition of H_2O_2 to O_2 followed by electroreduction of O_2 (four-electron process). It has been reported that the direct reduction is the preferred pathway for noble metal electrocatalysts [32]. The response process of the reduction of hydrogen peroxide on Pt/PPy hollow spheres mainly involved two steps. Hydrogen peroxide molecules firstly diffused and were absorbed on the surface of Pt NPs, followed by reaction with two electrons. The PPy shell mainly acts as an electron transporter providing conductivity between the electrode and Pt NPs as well as matrix to inhibit the aggregation of Pt NPs.

Fig. 5C shows the CVs of Pt/PPy hybrid microspheres modified electrode in the presence of H_2O_2 with different concentrations. With the increasing concentration of H_2O_2, the reduction peak current increases gradually (from −7.85 to −32.54 μA). The amperometric response of the modified electrode was investigated by successively adding a certain amount of H_2O_2 to a continuous stirring PBS solution (0.1 M, pH = 7.0). The typical *i*–*t* curve for the modified electrode is shown in Fig. 5D. As H_2O_2 was added into the stirring PBS, the modified electrode responded

Table 1
Comparison table for the different modified electrode.

Electrode	Detection potential (V vs Ag/AgCl)	LOD[a] (μM)	Response time[b] (s)	Reference
HRP/SGCCN	−0.25	12.89	<4c	[28]
HRP/nano-Au/SGCCN	−0.17[c]	6.1		[27]
HRP/TCAP/GC	−0.20	200	<10c	[26]
ZnO–GNPs–Nafion–HRP/GC	−0.30	9.0	<5c	[29]
HRP–AuNPs–SF/GC	−0.60[c]	5.0	<8d	[30]
Pt/PPy/GC	−0.10	1.2	<2c	Present work

SGCCN: sol–gel-derived ceramic-carbon nanotube; TCAP: 5,2′: 5′,2″-terthiophene-3′-carboxylic acid polymer; GNPs: gold nanoparticles; SF: silk fibroin.
[a] Limit of detection based on a signal-to-noise ratio of 3.
[b] The time required to reach the 95% (c) or 90% (d) steady-state response.
[c] The use of saturated calomel electrode (SCE) served as the reference electrode.

rapidly to the substrate with the sensitivity calculated to be 80.4 mA M^{-1} cm^{-2}. As shown in Table 1, the applied potential was more positive than certain HRP-based H_2O_2 sensors [26–30]. The Pt/PPy modified electrode could achieve the maximum steady-state current within 2 s, which was much shorter than the response time of certain HRP-based biosensors [26,28–30]. The calibration curve (inset of Fig. 5D) shows a linear response to H_2O_2 concentration in the range of 1.0–8.0 mM (correlation coefficient, 0.9965) with a detection limit of 1.2 μM based on a signal-to-noise ratio (S/N) of 3. The detection limit of Pt/PPy modified GCE was much lower than that of some HRP-based biosensors [26–30], indicating the high performance of our products modified electrode. From the comparison data mentioned above, it can be concluded that the as-synthesized ultra-high-density Pt-decorated PPy hollow spheres have good electrocatalytic activity towards H_2O_2.

4. Conclusions

In summary, we have successfully synthesized ultra-high-density Pt/PPy hybrid hollow microspheres by wet chemical method using Fe_3O_4 microspheres as template. Pt NPs are equably deposited on the PPy shell with the mean diameter of around 4.1 nm. It is found that GCE modified by the obtained Pt/PPy hybrid hollow microspheres exhibits superior electrocatalytic activity towards the reduction of H_2O_2. The modified electrode displays a relatively low reduction potential (−0.1 V), a fast response time (<2 s) and a relatively low detection limit of 1.2 μM (S/N = 3).

Acknowledgments

The work has been supported by National 973 Project (Nos. 2007CB936203 and S2009061009), NSF China (Nos. 50973038 and 50873045), and National 863 Project (No. 2007AA03Z324).

References

[1] E. Antolini, E.R. Gonzalez, Appl. Catal. A: Gen. 365 (2009) 1.
[2] X. Li, Y. Gao, J. Gong, L. Zhang, L.Y. Qu, J. Phys. Chem. C 113 (2009) 69.
[3] P. Xu, X.J. Han, C. Wang, D.H. Zhou, Z.S. Lv, A.H. Wen, X.H. Wang, B. Zhang, J. Phys. Chem. B 112 (2008) 10443.
[4] T.K. Chang, C.C. Chang, T.C. Wen, J. Power Sources 185 (2008) 603.
[5] Z.M. Peng, H. Yang, Nano Today 4 (2009) 143.
[6] Z.W. Chen, M. Waje, W.Z. Li, Y.S. Yan, Angew. Chem. Int. Ed. 46 (2007) 4060.
[7] L.Q. Rong, C. Yang, Q.Y. Qian, X.H. Xia, Talanta 72 (2007) 819.
[8] J.J. Yu, D.L. Yu, T. Zhao, B.Z. Zeng, Talanta 74 (2008) 1586.
[9] L.X. Zhang, L. Wang, S.J. Guo, J.F. Zhai, S.J. Dong, E.K. Wang, Electrochem. Commun. 11 (2009) 258.
[10] W. Yang, C. Yang, M. Sun, F. Yang, Y. Ma, Z.X. Zhang, X.R. Yang, Talanta 78 (2009) 557.
[11] Z.W. Chen, L.B. Xu, W.Z. Li, M. Waje, Y.S. Yan, Nanotechnology 17 (2006) 5254.
[12] S.J. Guo, S.J. Dong, E.K. Wang, Small 5 (2009) 1869.
[13] S.S. Kumar, C.S. Kumar, J. Mathiyarasu, K.L. Phani, Langmuir 23 (2007) 3401.
[14] Y.C. Liu, T.C. Chuang, J. Phys. Chem. B 107 (2003) 12383.
[15] K. Maksymiuk, Electroanalysis 18 (2006) 1537.
[16] R. Akinyeye, I. Michira, M. Sekota, A. Al-Ahmed, P. Baker, E. Iwuoha, Electroanalysis 18 (2006) 2441.
[17] L. Al-Mashat, H.D. Tran, W. Wlodarski, R.B. Kaner, K. Kalantar-zadeh, Sens. Actuators B: Chem. 134 (2008) 826.
[18] E. Pintér, R. Patakfalvi, T. Fü1lei, Z. Gingl, I. Dékány, C. Visy, J. Phys. Chem. B 109 (2005) 17474.
[19] S.V. Vasilyeva, M.A. Vorotyntsev, I. Bezverkhyy, E. Lesniewska, O. Heintz, R. Chassagnon, J. Phys. Chem. C 112 (2008) 19878.
[20] M. Sigaud, M. Li, S. Chardon-Noblat, F. José Cadete Santos Aires, Y. Soldo-Olivier, J.-P. Simon, A. Renouprez, A. Deronzier, J. Mater. Chem. 14 (2004) 2606.
[21] S. Mokrane, L. Makhloufi, N. Alonso-Vante, J. Solid State Electrochem. 12 (2008) 569.
[22] H.B. Zhao, L. Li, J. Yang, Y.M. Zhang, H. Li, Electrochem. Commun. 10 (2008) 876.
[23] H.B. Zhao, L. Li, J. Yang, Y.M. Zhang, J. Power Sources 184 (2008) 375.
[24] J. Li, X.Q. Lin, Microchem. J. 87 (2007) 41.
[25] L.H. Tang, Y.H. Zhu, L.H. Xu, X.L. Yang, C.Z. Li, Electroanalysis 19 (2007) 1677.
[26] Y.T. Kong, M. Boopathi, Y.B. Shim, Biosens. Bioelectron. 19 (2003) 227.
[27] C.X. Lei, S.Q. Hu, N. Gao, G.L. Shen, R.Q. Yu, Bioelectrochemistry 65 (2004) 33.
[28] H.J. Chen, S.J. Dong, Biosens. Bioelectron. 22 (2007) 1811.
[29] C.L. Xiang, Y.J. Zou, L.X. Sun, F. Xu, Sens. Actuators B: Chem. 136 (2009) 158.
[30] H.S. Yin, S.Y. Ai, W.J. Shi, L.S. Zhu, Sens. Actuators B: Chem. 137 (2009) 747.
[31] X.F. Lu, H. Mao, W.J. Zhang, Polym. Compos. 30 (2009) 847.
[32] D.X. Cao, L.M. Sun, G.L. Wang, Y.Z. Lv, M.L. Zhang, J. Electroanal. Chem. 621 (2008) 31.